Phytoplankton Community Structure and the Drawdown of Nutrients and CO_2 in the Southern Ocean

Kevin R. Arrigo, *et al.*

Science **283**, 365 (1999);
DOI: 10.1126/science.283.5400.365

ite (X_{Mg} = 1.0) and (ii) an unusually Fe-rich (X_{Mg} = 0.82) Ni-bearing [~3000 parts per million (ppm)] San Carlos olivine (*12*). For the wadsleyite diffusion experiments, we synthesized two samples of wadsleyite in multianvil experiments and characterized them by optical microscopy, x-ray diffraction, and electron microprobe analysis. In one case, single crystals of olivine ($X_{Mg} \approx 0.9$ and ~3000 ppm of Ni) from the Troodos ophiolite complex in Cyprus were transformed to wadsleyite of the same composition at 15 GPa and 1250°C; crystals in the form of (010) plates, with dimensions of 150 to 220 μm and containing occasional (010) twins, were obtained. The second sample was synthesized by transforming synthetic olivine powder ($X_{Mg} \approx 0.82$ and <100 ppm of Ni) at 16 GPa and 1800°C to polycrystalline wadsleyite with an average grain size of 60 to 100 μm.

7. The crystals were prepared for diffusion experiments by polishing surfaces (which were approximately perpendicular to [010], in the case of the single crystals) with a diamond polishing compound (0.25-μm grit size). Gold was used as the sample container because it is mechanically weak and prevents the crystals from being stressed or damaged during pressurization; also, unlike Pt, Au does not react chemically with the sample to cause a loss of Fe. The sample container was prepared by drilling a 250-μm-diameter hole in a Au wire that is 1 mm in diameter; the samples were placed together in this hole with the polished surfaces in contact. The capsule was closed by deforming the Au to obtain a cylinder with a length of 1 mm and a diameter of 1 mm, with the sample located at the center.
8. In the multianvil experiments [R. C. Liebermann and Y. Wang, in *High-Pressure Research: Applications to Earth and Planetary Sciences*, vol. 67 of *Geophysical Monograph Series*, Y. Syono and M. H. Manghnani, Eds. (American Geophysical Union, Washington, DC, 1992), pp. 19–31] a MgO octahedron with a 14-mm edge length was used as the pressure cell. A cylindrical $LaCrO_3$ heater with a stepped wall thickness was used to minimize thermal gradients. Temperature was measured with an axially located W3%Re/W25%Re thermocouple and was controlled to ±1°C during experiments that had durations of up to 24 hours. High pressure was generated using eight 32-mm cubic WC anvils with corners truncated to an edge length of 8 mm. Pressure was calibrated at 1000°C using phase transformations in SiO_2, Fe_2SiO_4, and Mg_2SiO_4 with an uncertainty of 0.5 GPa. After pressurization, temperature was raised to the desired value at a rate of 100°C/min; after the diffusion anneal, samples were quenched to <300°C in ~1 s. Because the distance between the thermocouple and sample was ~0.5 mm (Fig. 1), temperature errors due to thermal gradients are likely to be <20°C. [For further details, see D. C. Rubie, C. R. Ross, M. R. Carroll, S. C. Elphick, *Am. Mineral.* **78**, 574 (1993), and D. C. Rubie, S. Karato, H. Yan, H. St. C. O'Neill, *Phys. Chem. Miner.* **20**, 315 (1993).]
9. Oxygen fugacity is estimated by assuming that the Au capsule maintained a closed system and that the volume change of the samples on compression was negligible. Given the volume and composition of olivine, the free energy of the system is minimized to obtain the equilibrium oxygen fugacity [see R. Dohmen, S. Chakraborty, H. Palme, W. Rammensee, *Am. Mineral.* **83**, 970 (1998) for details]. Calculations with published thermodynamic data [R. A. Robie, B. S. Hemingway, J. R. Fisher, *U.S. Geol. Surv. Bull. 1452* (1979); D. R. Sull and H. Prophet, Eds., *JANAF Thermochemical Tables* (Government Printing Office, Washington, DC, ed. 3, 1971)] yield $f_{O_2} = 10^{-8}$ to 10^{-9} bars, which is about an order of magnitude lower than that of the wüstite-magnetite buffer at 1400°C and 15 GPa. Uncertainties in this estimate are mainly of consequence when comparing results of this study with data from previous studies at 1 bar (Fig. 2B).
10. Analyses were performed with Cameca SX-50 (Bayreuth) and JEOL 8900 RL (Köln) electron microprobes. Standards were silicates and oxides, and beam conditions were 15 kV and 15nA with counting times of 20 s.
11. For the polycrystalline wadsleyite, detailed element mapping was performed to define the boundary conditions under which diffusion occurred. Results show that contributions from grain boundary diffusion in the polycrystalline material (Fig. 1) can be neglected in the 1100°C experiment, and the diffusion process was therefore treated as volume diffusion between two initially homogeneous slabs. The appropriate solution to the diffusion equation [for example, J. Crank, *The Mathematics of Diffusion* (Oxford Univ. Press, Oxford, 1975), Eq. 2.14] was fit to the concentration profiles to determine the diffusion coefficient. In the experiment at 1200°C, grain boundary diffusion in the somewhat finer grained polycrystalline material contributed substantially to the diffusion process. In this case, a solution was used with a boundary condition that corresponded to a constant composition at the surface of the single crystal, as seen in the elemental concentration maps [J. Crank, *The Mathematics of Diffusion* (Oxford Univ. Press, Oxford, 1975), Eq. 3.13]. The difference in behavior of the two samples is related to the slight difference in grain size rather than to the temperature at which the samples were annealed. The solution for the single-crystal part is the same, irrespective of which equation is used to fit the data.
12. S. Chakraborty, *J. Geophys. Res.* **102**,12317 (1997).
13. Diffusion rates at $f_{O_2} = 10^{-8}$ bar were calculated with the measured dependency of diffusion rates on oxygen fugacity ($D \propto f_{O_2}^{1/6}$) as reported by D. K. Buening and P. R. Buseck, *ibid.* **78**, 6852 (1973), and A. Nakamura and H. Schmalzried, *Ber. Bunsenges. Phys. Chem.* **88**, 140 (1984). Recent unpublished data from our laboratory are consistent with the dependencies found by these authors.
14. S. Chakraborty and J. Ganguly, *Contrib. Mineral. Petrol.* **111**, 74 (1992); J. Ganguly, W. Cheng, S. Chakraborty, *ibid.* **131**, 171 (1998).
15. Y. Xu, B. T. Poe, T. J. Shankland, D. C. Rubie, *Science* **280**, 1415 (1998).
16. Measured Fe^{3+} contents of wadsleyite are typically 0.03 to 0.04 weight % as opposed to <0.01 weight % in olivine when total Fe contents are similar (*23*).
17. The shortest Mg-Mg distances in Mg_2SiO_4 olivine are 2.99 Å [K. Fujino, S. Sasaki, Y. Takeuchi, R. Sadanaga, *Acta Crystallogr.* **B37**, 513 (1981)], whereas in wadsleyite, there are many distances between 2.80 and 3.06 Å [H. Horiuchi and H. Sawamoto, *Am. Mineral.* **66**, 568 (1981)].
18. The electrical conductivities of wadsleyite and ringwoodite are almost identical (*15*), and these phases also have similar Fe^{3+} contents (*23*).
19. A similar conclusion was reached by Farber *et al.*, but they probably overestimated the effect by two orders of magnitude (*22*).
20. L. H. Kellogg and D. L. Turcotte, *J. Geophys. Res.* **95**, 421 (1990).
21. S. J. Mackwell, D. Dimos, D. L. Kohlstedt, *Philos. Mag. A* **57**, 779 (1988); B. J. Wanamaker, *Geophys. Res. Lett.* **21**, 21 (1994).
22. D. L. Farber, Q. Williams, F. J. Ryerson, *Nature* **371**, 693 (1994).
23. H. St. C. O'Neill *et al.*, *Am. Mineral.* **78**, 456 (1993).
24. This research was partly supported by the European Union's TMR–Large Scale Facilities Programme (contract ERBFMGECT980111) and the Natural Environment Research Council (grant NERC GR9/03066).

21 September 1998; accepted 18 November 1998

Phytoplankton Community Structure and the Drawdown of Nutrients and CO_2 in the Southern Ocean

Kevin R. Arrigo,* Dale H. Robinson, Denise L. Worthen, Robert B. Dunbar, Giacomo R. DiTullio, Michael VanWoert, Michael P. Lizotte

Data from recent oceanographic cruises show that phytoplankton community structure in the Ross Sea is related to mixed layer depth. Diatoms dominate in highly stratified waters, whereas *Phaeocystis antarctica* assemblages dominate where waters are more deeply mixed. The drawdown of both carbon dioxide (CO_2) and nitrate per mole of phosphate and the rate of new production by diatoms are much lower than that measured for *P. antarctica*. Consequently, the capacity of the biological community to draw down atmospheric CO_2 and transport it to the deep ocean could diminish dramatically if predicted increases in upper ocean stratification due to climate warming should occur.

Climate models (*1*) indicate that over the next half century, the Southern Ocean carbon (C)cycle will change dramatically in response to rising atmospheric CO_2. Increased precipitation is predicted to intensify surface ocean stratification, thereby decreasing the downward flux of C and reducing the capacity of the Southern Ocean to take up anthropogenic CO_2. The biological response to the predicted changes in ocean dynamics is poorly understood. Here we present results from the oceanographic program Research on Ocean-Atmosphere Variability and Ecosystem Response in the Ross Sea (ROAVERRS), cruise NBP96-6 (*2*), that show how increased stratification in the Ross Sea would affect phytoplankton community structure and CO_2 and nutrient drawdown in the Ross Sea.

Three spatially distinct phytoplankton assemblages (*3*) dominated the the Ross Sea during 1996–97, with phytoplankton community structure varying as a function of the depth of the mixed layer. The assemblage with the widest distribution and highest biomass of chlorophyll a (Fig. 1A) was dominated by *Phaeocystis antarctica* and extended from the Ross Ice Shelf northward to 75°S (Fig. 1B). Mixed layers in the *P. antarctica*–

dominated region were typically 25 to 50 m deep (Fig. 1C) and were relatively weakly stratified (Fig. 2). Although seawater density is controlled primarily by salinity at the low temperatures typical of this region (–1.85° to 2°C), the vertical structure of seawater temperature (*4*) mirrored that of density. *P. antarctica* phytoplankton dominated in the more deeply mixed waters because of their ability to maintain near-maximal photosynthetic rates at much lower irradiance levels than do diatoms (69 and 121 μmol of photons m^{-2} s^{-1}, respectively, during this study).

Diatoms, primarily the pennate form *Nitzschia subcurvata*, were dominant farther north and west and in Terra Nova Bay, where recent sea ice melt resulted in mixed layers (5 to 20 m) that were both much shallower (Fig. 1C) and more strongly stratified (Fig. 2) than in those areas where *P. antarctica* was most abundant. During the early stages (20–21 December 1996) of the phytoplankton bloom in Terra Nova Bay, diatoms and *P. antarctica* were about equally abundant, composing 60 and 40% of the phytoplankton biomass, respectively. Later (4–5 January 1997), after stratification had intensified and the mixed layer had shoaled, samples taken along the same transect showed that diatoms had become dominant in this environment of greater light, ultimately accounting for >90% of phytoplankton biomass. *Phaeocystis* sp. and diatoms are the dominant phytoplankton taxa throughout Antarctic and Arctic waters (*5*).

A small near-shore cryptophyte bloom also was observed in the upper 20 m of the water column within the coastal polynya (area of open water surrounded by sea ice) between 76.0°S and 76.5°S (Fig. 1B). Because of the small number of stations at which cryptophytes dominated, they have been excluded from further discussion.

Waters dominated by diatoms and *P. antarctica* differed markedly with respect to their nutrient drawdown characteristics. In general, phytoplankton remove N and P from the environment in molar ratios near the Redfield ratio (N:P = 16). Disappearance ratios calculated from the slope of nitrate (NO_3) plotted against phosphate (PO_4) for the entire ROAVERRS NBP96-6 data set (14.9 ± 0.45) are consistent with Redfield uptake kinetics (Table 1 and Fig. 3A). However, when samples dominated by either diatoms or *P. antarctica* were analyzed independently, a different pattern emerged. Disappearance ratios of NO_3:PO_4 were significantly different ($P < 0.001$) for these two phytoplankton taxa (Table 1 and Fig. 3B): The ratio for *P. antarctica* (19.2 ± 0.61) was nearly twice as high as that for diatoms (9.69 ± 0.33). In samples with a mixed phytoplankton assemblage, the NO_3:PO_4 disappearance ratio was intermediate between these two extremes. Furthermore, the plot of NO_3 versus PO_4 concentration shows that the maximum standing crop attainable by the two phytoplankton taxa would be determined by the availability of different nutrients—NO_3 in the case of *P. antarctica* and PO_4 for diatoms. Because pre-bloom nutrient concentrations were uniform throughout the Ross Sea (as indicated by the intersecting lines in Fig. 3B), the variation in disappearance ratios reflected taxonomic differences in nutrient drawdown and not chemical differences in the water masses where each taxon dominated.

Phaeocystis antarctica and diatoms also exhibited different ratios of C to nutrient drawdown. For example, the disappearance ratio of total dissolved inorganic C (TDIC) to PO_4 was significantly higher ($P < 0.001$) for *P. antarctica* (147 ± 26.7) than for diatoms (94.3 ± 20.1) (Table 1). Assuming that any reduction in TDIC was a result of drawdown of CO_2 by phytoplankton, then the ROAVERRS NBP96-6 data suggest that for every mole of PO_4 removed from the water column, *P. antarctica* took up 56% more CO_2 than did diatoms. In contrast, the disappearance ratio TDIC:NO_3 was higher for diatoms (9.23 ± 1.66) than for *P. antarctica* (7.81 ± 1.32), although the difference was not statistically significant (at the 95% confidence level). The TDIC:NO_3 disappearance ratio for diatoms also was significant-

K. R. Arrigo, NASA Goddard Space Flight Center, Code 971.0, Greenbelt, MD 20771, USA. D. H. Robinson. Romberg Tiburon Center for Environmental Studies, San Francisco State University, 3150 Paradise Drive, Post Office Box 855, Tiburon, CA 94920–0855, USA. D. L. Worthen, Science Systems and Applications, Lanham, MD 20706, USA. R. B. Dunbar, Geological and Environmental Sciences, Stanford University, Stanford, CA 94305–2115, USA. G. R. DiTullio, University of Charleston, Grice Marine Laboratory, 205 Fort Johnson, Charleston, SC 29412, USA. M. VanWoert, National Oceanic and Atmospheric Administration, NESDIS, E/RA3 World Weather Building, 4700 Silver Hill Road, Washington, DC 20233–9910, USA. M. P. Lizotte, Department of Biology and Microbiology, University of Wisconsin Oshkosh, Oshkosh, WI 54901, USA.

*To whom correspondence should be addressed.

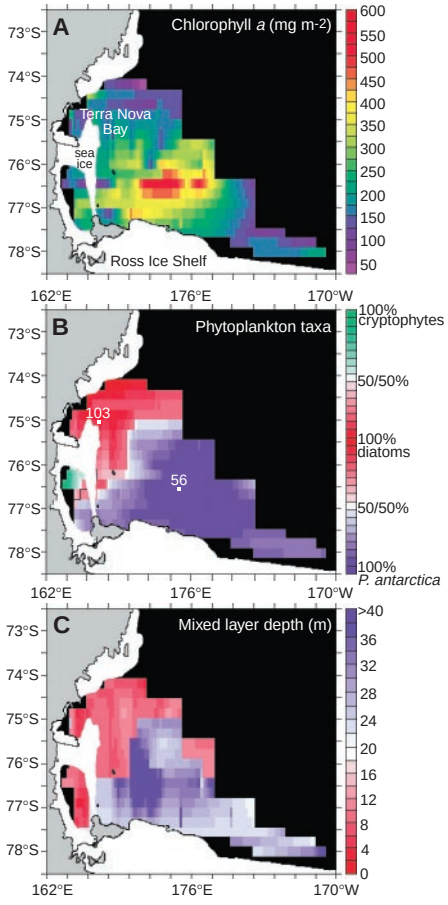

Fig. 1. Horizontal distributions of (**A**) chlorophyll a, (**B**) phytoplankton taxa (stations 56 and 103 denote the location of the vertical density profiles shown in Fig. 2), and (**C**) mixed layer depth in the surface of the Ross Sea measured during ROAVERRS cruise NBP96-6.

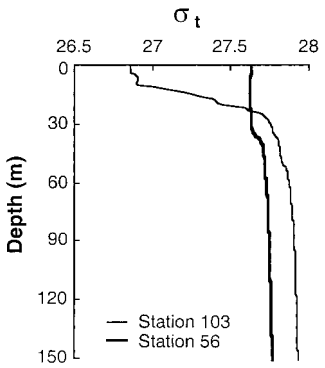

Fig. 2. Density profiles at stations 56 and 103 (see Fig. 1B for locations). Station 56 was dominated by *P. antarctica*, whereas station 103 was dominated by diatoms.

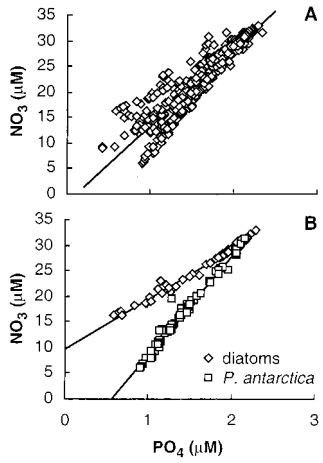

Fig. 3. Plots of nitrate concentration versus phosphate concentration in the Ross Sea measured during ROAVERRS cruise NBP96-6. (**A**) shows all ROAVERRS NBP96-6 samples, including those with mixed phytoplankton populations containing both diatoms and *P. antarctica*, and (**B**) shows samples in which diatoms and *P. antarctica* overwhelmingly dominated the phytoplankton population, accounting for >85 and >90%, respectively, of total phytoplankton biomass.

ly higher ($P < 0.001$) than their ratio of cellular particulate organic C to particulate N (POC:PN) (6.37 ± 0.36), which suggests either that 31% of the C fixed by diatoms was released as dissolved organic C (DOC) or that a similar percentage of their total N requirement was being satisfied by a source other than NO_3. DOC has been reported to be unusually low in the Ross Sea (*6*), accounting for only about 11% of total fixed C, which indicates that DOC production was not the cause of the observed difference between the TDIC:NO_3 disappearance ratio and the cellular POC:PN ratio in diatoms.

Although N metabolism was not assessed during ROAVERRS cruise NBP96-6, indirect evidence suggests that the use of other N sources by diatoms is the likely explanation for the difference between the TDIC:NO_3 and POC:PN ratios. First, concentrations of NH_4, the likely supplemental N source, were as high as 1.1 μM (mean = 0.14 ± 0.18 μM) in waters dominated by diatoms, probably the result of zooplankton grazing. This inference is supported in diatom-dominated waters by the relatively high concentrations of chlorophyll degradation products (phaeophorbides) that are indicative of grazing (*7*). Second, the disappearance ratio for $Si(OH)_4$:NO_3, expected to be 1 for diatoms living exclusively on NO_3, was only 0.47 ± 0.03 ($n = 56$). This low value suggests that regeneration of N was proceeding at rates much greater than that of biogenic silica (*8*) and that the diatoms were using this recycled N, either because it is energetically favored over NO_3 (*8*) or because diatoms had a diminished capacity to take up NO_3 because of iron limitation (*9*). Finally, accounting for the presumed NH_4 uptake by diatoms yields a disappearance ratio of (NH_4 + NO_3):PO_4 (14.1) that is closer to the Redfield ratio than to the NO_3:PO_4 disappearance ratio.

In contrast to waters dominated by diatoms, those dominated by *P. antarctica* exhibited a TDIC:NO_3 disappearance ratio (7.81 ± 1.32) that was nearly identical to their POC:PN ratio (7.71 ± 0.53). This result indicates that the N requirement of *P. antarctica* was being satisfied entirely by NO_3. Rates of nutrient regeneration and recycling appear to have been much lower in these waters than in the diatom-dominated waters of the Ross Sea. Rates of daily production were similar between these two phytoplankton assemblages, averaging 1.33 ± 0.64 and 1.35 ± 0.63 g of C m^{-2} d^{-1} for *P. antarctica* and diatoms, respectively. However, because of the nearly complete reliance of *P. antarctica* on new N sources, the amount of production available for export out of the upper ocean was 43% greater when the phytoplankton community was dominated by *P. antarctica* (1.33 g of C m^{-2} d^{-1}) than when dominated by diatoms (0.93 g of C m^{-2} d^{-1}).

Although transient changes in the Redfield ratios of phytoplankton are commonly observed in systems that experience depletion of one or more nutrients (*10*), large taxonomic differences in nutrient drawdown ratios were not expected in the Southern Ocean, where inorganic macronutrients are almost always in ample supply. Taxonomic variation in NO_3:PO_4 disappearance ratios can be explained by differences in N dynamics between diatom and *P. antarctica* assemblages, but taxonomic differences in TDIC:PO_4 disappearance ratios are not as well understood (they may result from different P requirements). Nevertheless, taxonomic differences in C:P uptake ratios have important implications for climate models that include biology. In such models, it is generally assumed that CO_2 is drawn down by phytoplankton in constant proportion to the removal of PO_4 until PO_4 is exhausted (*1*). The ROAVERRS NBP96-6 data imply that these models underestimate CO_2 drawdown wherever the spring phytoplankton bloom is dominated by *P. antarctica*, which has a TDIC:PO_4 disappearance ratio 40% higher than the Redfield C:P ratio. Should the community shift from *P. antarctica* to diatom dominance in response to enhanced upper ocean stratification or some other environmental factor, then the CO_2 drawdown estimated from the C:P ratio would drop by 36%.

Table 1. Elemental ratios measured during ROAVERRS cruise NBP96-6. CI, confidence interval.

	Slope ± 95% CI	R^2	N	P value
All data				
TDIC:PO_4 (m:m)	111.4 ± 7.9	0.74	293	<0.001
NO_3:PO_4 (m:m)	14.9 ± 0.45	0.88	552	<0.001
TDIC:NO_3 (m:m)	7.82 ± 0.43	0.80	312	<0.001
POC:PN (m:m)	7.13 ± 0.13	0.95	565	<0.001
Diatoms				
TDIC:PO_4 (m:m)	*94.3 ± 20.1	0.74	34	<0.001
NO_3:PO_4 (m:m)	*9.69 ± 0.33	0.99	44	<0.001
TDIC:NO_3 (m:m)	9.23 ± 1.66	0.79	38	<0.001
POC:PN (m:m)	*6.37 ± 0.36	0.96	51	<0.001
P. antarctica				
TDIC:PO_4 (m:m)	*147 ± 26.7	0.73	47	<0.001
NO_3:PO_4 (m:m)	*19.2 ± 0.61	0.98	80	<0.001
TDIC:NO_3 (m:m)	7.81 ± 1.32	0.75	50	<0.001
POC:PN (m:m)	*7.71 ± 0.53	0.90	92	<0.001

*Denotes significant difference between diatom- and *P. antarctica*–dominated waters at the 95% confidence level.

References and Notes

1. J. L. Sarmiento *et al.*, *Nature* **393**, 245 (1998).
2. During the ROAVERRS cruise NBP96-6, 108 hydrographic stations within the Ross Sea (from 163°E to 170°W and from 72°S to 78°S) were sampled aboard the research vessel *Nathaniel B. Palmer* between 16 December 1996 and 8 January 1997. At each station, a rosette of 10-liter Bullister Bottles was used to collect water samples from between five and eight discrete depths within the upper 150 m of the water column. Subsamples were taken for quantification of phytoplankton pigments, inorganic macronutrients, particulate C and N, and TDIC. The rosette also included instrumentation for measuring conductivity and temperature (Sea Bird Electronics) for determination of mixed layer depth [defined as the depth where density (σ_t) is 0.02 greater than surface values]. Suspended particles were collected by filtration of water samples through Whatman GF/F glass fiber filters for analysis of pigment composition and concentration by high-performance liquid chromatography, with the method described in (*9*) as modified from (*11*). Inorganic macronutrient concentrations were determined on board ship with a Technicon AutoAnalyzer II system. Particulate organic C and particulate N samples were measured according to the Joint Global Ocean Flux Study (JGOFS) protocols in. TDIC was measured by thermal conductivity analysis of CO_2 in a helium carrier gas stream after stripping within a bubbler system upon acidification. Water samples were collected from rosette bottles according to JGOFS gas sampling protocols. Analysis of replicate 5-ml aliquots was typically completed within several hours. The stripping procedure is similar to that commonly used for stable isotopic studies, in which the separated CO_2 gas is quantitatively retained for shore-based isotopic analysis. In our modification, we ported the effluent carrier gas and the CO_2 stream through a gas chromatograph with a thermal conductivity detector (modified Carlo-Erba series NA-1100). Standardization was done with Scripps Institution of Oceanography seawater standards supplied by A. Dickson. Based on replicate analyses, our precision (1 SD) was 15 μM kg^{-1}, or about 0.65%. TDIC drawdown in the upper water column during ROAVERRS cruise NBP96-6 ranged from 20 to 200 μM kg^{-1}, or 1 to 9%.
3. Three marker pigments were used for determining distributions of the major phytoplankton taxa: fucoxanthin for diatoms, 19′-hexanolyoxyfucoxanthin for haptophytes (primarily *P. antarctica*), and alloxanthin for cryptophytes. In samples dominated by each of these phytoplankton taxa, the molar ratio of the corresponding marker pigment to chlorophyll a was approximately 1:1. Therefore, the relative abundance of each phytoplankton taxon in terms of chlorophyll a could be calculated as the marker pigment concentration divided by the sum of all three marker pigments. Taxonomic identifications were confirmed by microscopy.
4. K. R. Arrigo *et al.*, data not shown.
5. S. Z. El-Sayed and G. A. Fryxell, in *Antarctic Microbiology*, E. I. Friedmann, Ed. (Wiley-Liss, New York, 1993), pp. 65–122.
6. C. A Carlson *et al.*, *Limnol. Oceanogr.* **43**, 375 (1998).
7. G. R. DiTullio and W. O. Smith Jr., *J. Geophys. Res.* **101**, 18,467 (1996)
8. R. C. Dugdale and F. P. Wilkerson, *Nature* **391**, 270 (1998).
9. D. A. Huchins and K. W. Bruland, *ibid.* **393**, 561 (1998); P. N. Sedwick and G. R. DiTullio, *Geophys. Res. Lett.* **24**, 2515 (1997).
10. R. N. Sambrotto *et al.*, *Nature* **363**, 248 (1993).
11. S. W Wright *et al.*, *Mar. Ecol. Prog. Ser.* **77**, 183 (1991).

12. We thank A. Leventer for microscopic species identification, E. Quiroz for performing nutrient analyses, W. O. Smith Jr. for analyzing our CHN samples, and H. Rowe for running samples for TDIC. This work was supported by the Office of Polar Programs of NSF.

12 August 1998; accepted 23 October 1998